Ferromagnetic-resonance studies of epitaxial Ni, Co, and Fe films grown on Cu(100)/Si(100)

R. Naik, C. Kota, J. S. Payson, and G. L. Dunifer
Department of Physics and Astronomy, Wayne State University, Detroit, Michigan 48202
(Received 7 December 1992; revised manuscript received 11 February 1993)

Epitaxial films of Ni, Co, and Fe of thickness (10–500 Å) have been studied on Cu(100) seed layers grown at room temperature on Si(100) substrates freshly etched in a hydrofluoric acid solution. X-ray diffraction and reflection high-energy electron-diffraction measurements confirm the epitaxial growth of Ni and Co on Cu(100) with a fcc(100) structure, whereas Fe grows with a bcc(110) Pitsch orientation relationship. Ferromagnetic-resonance measurements have been used to study the in-plane and out-of-plane magnetic anisotropies of these films. Experimental data were fitted by using energy-density expressions that include uniaxial perpendicular anisotropy and bulk cubic anisotropy terms. Ni films with thicknesses < 100 Å show strong perpendicular magnetic anisotropy, which is attributed to a tetragonal deformation of the Ni lattice.

INTRODUCTION

Ferromagnetic-resonance (FMR) measurements have proven very useful for providing information on magnetic anisotropies in thin ferromagnetic films and multilayers.[1–11] FMR on multilayered films show multiple resonances whose origin is not yet clearly understood.[8–11] A useful approach for understanding the multiple resonances of the multilayer films may be to understand the measurements on single-layered films and then study the evolution of the FMR as one increases the number of layers. Single magnetic thin films have shown a broad range of magnetic properties which depend not only on thickness but also on the growth conditions, such as the deposition method, substrates used, their preparation, and the substrate temperature during the growth process. Magnetic properties have been found to be sensitive to the microstructure of the film as well as to the interface with a nonmagnetic layer, due to interfacial diffusion, roughness, and strain.[12,13] Much of the recent work has been aimed at improving the understanding of the magnetic anisotropy, especially when the easy axis of magnetization is oriented perpendicular to the plane of the film.[7,13] At present, we are unaware of any first-principle calculations of the perpendicular anisotropy for arbitrarily layered systems. As a result, experimentalists are guided by phenomenological approaches which consider contributions to the magnetic anisotropy from the magnetocrystalline, magnetoelastic, and demagnetization energies.

Epitaxial growth of magnetic metals on appropriate substrates has greatly facilitated the experimental determination of the magnetic anisotropies. Recently, it has been shown that wet-chemical etching of Si substrates with hydrofluoric acid (HF) solutions produce hydrogen-terminated surfaces which are highly ordered and relatively clean.[14] This allows epitaxial growth of Cu(100) on freshly HF-etched Si(100) substrates at room temperature.[15] Using the epitaxial Cu(100) film as a seed layer, several other metallic epitaxial films have also been grown.[16] In the present work, we used an epitaxial Cu(100) film on Si(100) as a seed layer in order to study the growth and magnetic properties of epitaxial Ni, Co, and Fe films for thicknesses ranging from 10–500 Å. Reflection high-energy electron diffraction (RHEED) was used to monitor the growth, quality, and structure of the films. The in-plane and out-of-plane magnetic anisotropies of these films were studied by measuring the resonant field of the FMR as a function of the dc magnetic-field orientation in the plane of the film and in a plane perpendicular to the film, respectively.

EXPERIMENTAL PROCEDURE

The films were grown in an ultrahigh vacuum using a molecular beam epitaxy (MBE) deposition system with a base pressure of 2×10^{-10} Torr. The growth chamber is equipped with a RHEED unit and two independent *e*-beam evaporators with computer-controlled pneumatic shutters. The sample can be rotated 360° with respect to the RHEED electron beam allowing one to study the full azimuthal dependence of the RHEED pattern. The rate of deposition and total thickness are measured with quartz thickness monitors calibrated using a diamond-stylus profilometer. The deposition rates were 0.5–1 Å/s. During deposition, the pressure was maintained at 2×10^{-9} Torr with the aid of a liquid-N_2 cryoshroud. A sample load-lock chamber connects a surface-analysis chamber to the growth chamber. The surface-analysis chamber is equipped with an Auger spectrometer and a reverse-view low-energy electron diffraction (LEED) unit.

Si(100) *p*-type substrates (1 cm^2) were degreased and etched in a 10% HF-deionized-water solution, pull dried, and loaded into the load-lock chamber. After pumping for about 2 h, the substrates were transferred into the growth chamber. The quality of the Si(100) surface was then observed using RHEED, which showed sharp streaky patterns along with Kikuchi lines, indicating a clean surface. Some of the substrates were further analyzed with LEED and Auger spectroscopy. LEED showed sharp spots and the Auger spectra showed no trace of oxygen. The RHEED patterns were continuously monitored during the deposition to study the quality

0163-1829/93/48(2)/1008(6)/$06.00

and structure of the Cu seed layer as well as the magnetic metals. All the films had a 50 Å Cu cap layer for protection from oxidation.

The FMR data were taken at room temperature using standard magnetic-resonance techniques. The microwave reflection spectrometer operates at a frequency of 12 GHz and employs magnetic-field modulation with phase-sensitive detection so that the detected signal is proportional to the field derivative of the absorbed power. The dc magnetic field, provided by a 12-in. Varian electromagnet, has a range of 0–13 kG and can be rotated in the horizontal plane through a total angle of 360°. The sample is mounted in a TE_{101} rectangular cavity on either a vertical side wall for "out-of-plane" measurements or on the bottom wall for "in-plane" measurements. Typical FMR samples were 4 mm×4 mm and were aligned via cleavage faces of the Si substrate. Standard θ-2θ x-ray diffraction scans were performed with Cu K_α radiation.

RESULTS AND DISCUSSION

In-plane x-ray diffraction studies have shown that Cu grows epitaxially on Si(100) at room temperature with a 45° rotation of the Cu lattice with respect to the Si(100) lattice.[17] Upon the initiation of Cu deposition, we observe that the sharp RHEED streaks of the Si(100) surface are replaced by broad and rather diffuse spots. For film thicknesses greater than about 150 Å, sharp elongated spots appear indicating that the growth of Cu is epitaxial but dominated by three-dimensional growth. Cross-sectional transmission electron microscopy (TEM) studies of a 1500-Å-thick Cu film indicate an intermixed region of Si and Cu of approximately 150 Å at the interface.[18] The role that the interfacial layer plays on the epitaxial growth of the Cu is not well understood. Figure 1(a) shows the RHEED pattern from a clean Si(100) substrate along a Si⟨110⟩ azimuth, whereas Fig. 1(b) shows the pattern along the same azimuth of Si after a 500-Å Cu deposition. There is also evidence of a polycrystalline component, as indicated by faint arcs. The RHEED patterns confirm the full fourfold azimuthal symmetry of the Cu(100) lattice and its 45° rotation with respect to the Si(100) lattice. Since the patterns do not change appreciably for Cu thicknesses greater than 500 Å, we chose a thickness of 500 Å as a seed layer for most of the films in order to study the subsequent growth of magnetic metals.

Growth of 10–500 Å of Ni or Co on the Cu seed layer maintained a similar RHEED pattern, indicating the same in-plane epitaxy as that of Cu. For example, Figs. 1(c) and 1(d) display the RHEED patterns of 500 Å of Co and 500 Å of Ni, respectively, deposited on a Cu(100) seed layer. Standard θ-2θ x-ray diffraction scans of 500-Å-thick Fe, Ni, and Co samples are shown in Fig. 2. The Ni and Co samples show only fcc(200) peaks. It is interesting to note the lack of a hcp Co phase (observed in the bulk), which would have appeared around $2\theta=44.5°$. The x-ray and RHEED data reveal that both Ni and Co have fcc (100) structures, rotated 45° from the Si(100) lattice. Knowing this epitaxial relationship allows one to find the magnetocrystalline anisotropies for the Ni and Co films using FMR. On the other hand, the growth of Fe on Cu(100) developed a significantly different RHEED pattern, to be described in the next paragraph. Since x-ray diffraction of the 500-Å Fe sample showed only the bcc(110) peak, this system provides an opportunity to study the growth of a bcc metal on a fcc metal.

The RHEED pattern for Fe, shown in Fig. 3, is quite complex. The initial 10–20 Å growth of Fe produces a broad and diffuse pattern and seems to have a fcc(100) structure. This is consistent with a previous report[19] in which Fe was found to adopt a fcc structure for thicknesses up to approximately 20 Å. This pattern changes for Fe thicknesses >20 Å and develops into a well-defined pattern around 100 Å, which remains essentially unchanged for a thickness up to 1500 Å. The RHEED patterns reveal fourfold azimuthal symmetry. These RHEED observations can be explained by the formation of a bcc-Fe(110) structure on a fcc(100) crystal using four of the 12 variants of the Pitsch orientation rela-

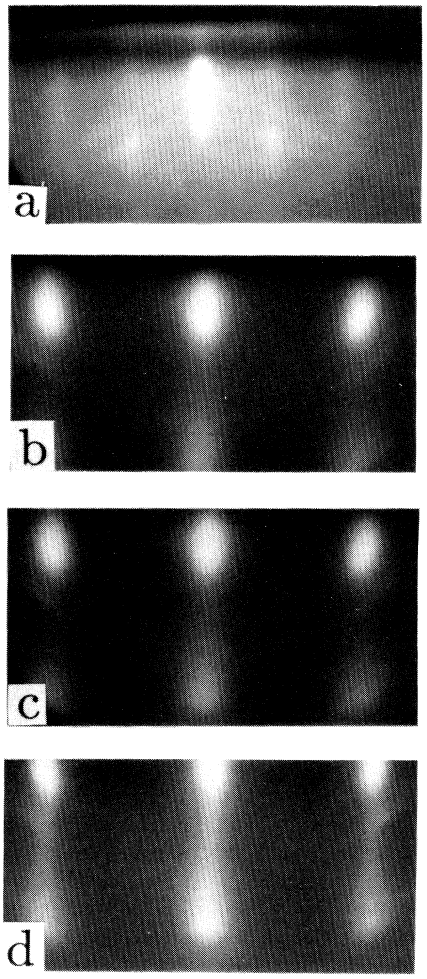

FIG. 1. RHEED patterns: (a) obtained from a clean Si(100) surface, (b) after a 500-Å Cu deposition, (c) after a 500-Å Co deposition on a 500-Å Cu seed layer, and (d) after a 500-Å Ni deposition on a 500-Å Cu seed layer. All patterns are taken along a Si⟨110⟩ azimuth with an electron beam of energy 15 keV.

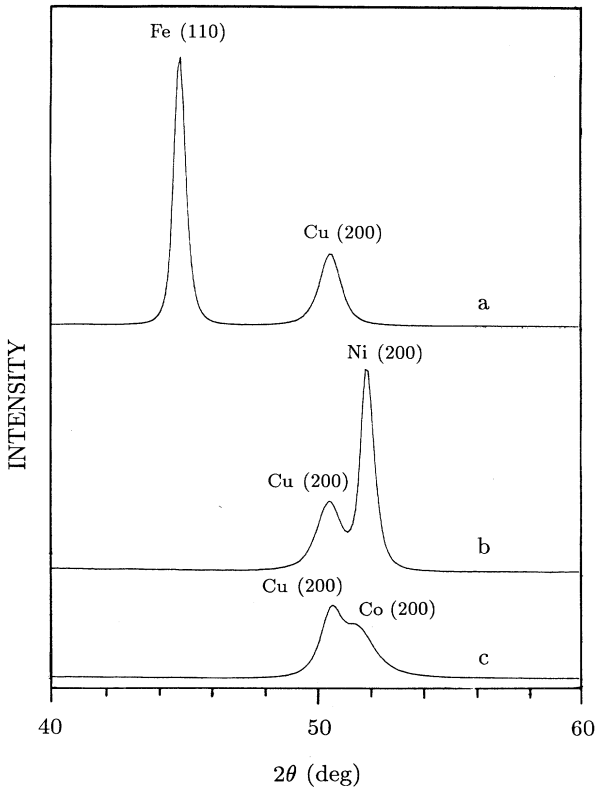

FIG. 2. X-ray diffraction scans (Cu K_α) for (a) 500 Å Fe, (b) 500 Å Ni, and (c) 500 Å Co. The samples were grown on a seed layer of 500-Å Cu(100)/Si(100).

tionships (OR).[20,21] The corresponding atomic arrangement at the fcc/bcc interface is shown in Fig. 4. The parallel planes are $(100)_f \| (110)_b$, and the parallel directions are $[011]_f \| [1\bar{1}1]_b, [0\bar{1}1]_f \| [\bar{1}11]_b, [0\bar{1}1]_f \| [1\bar{1}1]_b$, and $[011]_f \| [\bar{1}11]_b$, where the subscripts f and b represent fcc and bcc structures, respectively. This arrangement is the same as that predicted theoretically by the invariant line condition.[22] A more-detailed analysis of the RHEED observations along with TEM studies will be published separately.[23]

An analysis of the in-plane FMR measurements on all the samples agrees with the RHEED studies in confirming the various crystallographic directions of the magnetic metal. The angular dependence of the FMR for 500-Å Ni, Co, and Fe films is shown in Fig. 5. The direction of the easy magnetization axes in both Ni and Co is along the direction ⟨110⟩. This agrees with recent magnetization studies on similar films.[24,25] For Fe, with Pitsch OR, the easy and hard magnetic axes are parallel to the Cu⟨100⟩ and ⟨110⟩ directions, respectively. The dotted curves shown in the figure represent a theoretical fit to the data, making use of the following expression for the energy density E of a magnetic single-crystal film which includes contributions from the Zeeman, cubic anisotropy, and demagnetization factors:

$$E = -\mathbf{M}\cdot\mathbf{H} + K_1(\alpha_1^2\alpha_2^2 + \alpha_2^2\alpha_3^2 + \alpha_3^2\alpha_1^2) + (2\pi M^2 - K_u)\alpha_2^2 , \quad (1)$$

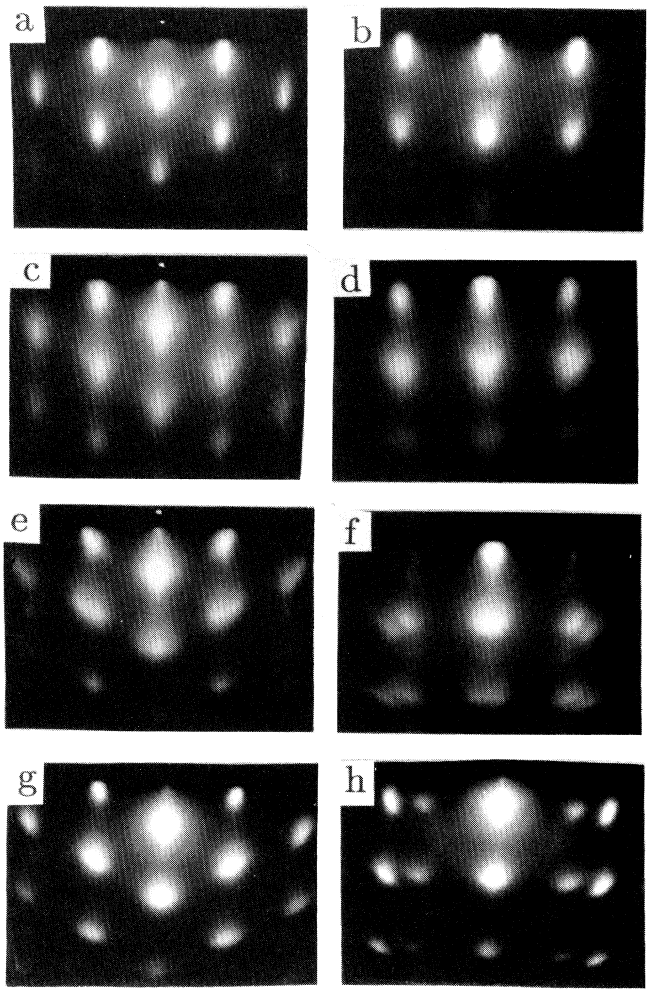

FIG. 3. RHEED data for an Fe deposition on Cu(100)/Si(100). (a) and (b) show patterns for a 1500-Å Cu(100) seed layer; (c) and (d) after a 10-Å Fe deposition; (e) and (f) after a 50-Å Fe deposition; (g) and (h) after a 500-Å Fe deposition. (a), (c), (e), and (g) are along a Si⟨100⟩ azimuth; (b), (d), (f), and (h) are along a Si⟨110⟩ azimuth.

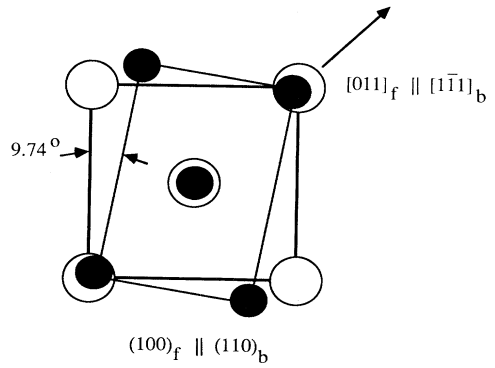

FIG. 4. The matching between fcc (open circles) and bcc (solid circles) lattices representing one of the four equivalent variants of the Pitsch OR.

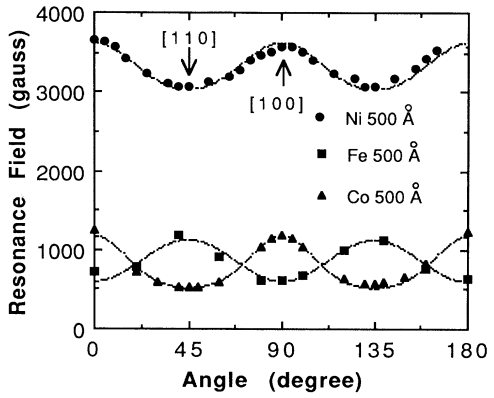

FIG. 5. The in-plane angular dependence of the 12-GHz FMR resonance fields for 500-Å Ni, Co, and Fe samples grown on Cu(100)/Si(100). The dotted curves were generated using the parameters given in Table I.

where K_1 is the usual fourth-order cubic magnetic crystalline anisotropy constant, K_u accounts for any perpendicular anisotropy, and α_i are the direction cosines of **M**. The film plane is taken parallel to the xz plane. The in-plane FMR resonant condition for a $\langle 100 \rangle$ surface orientation, including the noncollinearity of **M** and **H**, is given by[26]

$$(\omega/\gamma)^2=[H\cos(\phi_H-\phi)+4\pi M_{\rm eff}+(K_1/M)(2-\sin^2 2\phi)]\times[H\cos(\phi_H-\phi)+(2K_1/M)\cos 4\phi] . \quad (2)$$

The equilibrium condition is

$$H\sin(\phi_H-\phi)=(K_1/2M)\sin 4\phi , \quad (3)$$

where $\gamma=g|e|/(2mc)$ and $4\pi M_{\rm eff}=4\pi M-2K_u/M$. The angles ϕ_H and ϕ describe the orientation of **H** and **M**, respectively, referenced to an in-plane $\langle 100 \rangle$ direction.

For out-of-plane FMR measurements, the coordinate system used in our calculations is shown in Fig. 6. Since

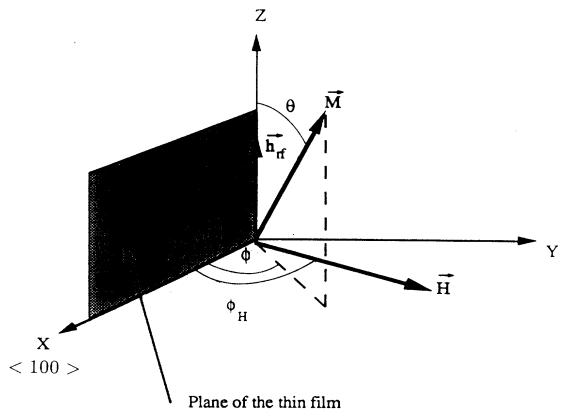

FIG. 6. The orientation of the dc magnetic field **H** and the magnetization **M** with respect to the coordinate system used in the calculations for the out-of-plane FMR measurements.

the dc field **H** is applied in the xy plane, the static equilibrium orientation of the magnetization is given by $\theta=\pi/2$ and

$$H\sin(\phi_H-\phi)=4\pi M_{\rm eff}\sin(\phi)\cos(\phi)+(K_1/2M)\sin 4\phi . \quad (4)$$

These two conditions are derived from Eq. (1) by using the equilibrium conditions that $\partial E/\partial\theta=0$ and $\partial E/\partial\phi=0$. The resonance field can then be calculated from an equation derived by Smit and Beljers:[27]

$$\left[\frac{\omega}{\gamma}\right]^2=\frac{1}{M^2\sin^2\theta}\left[\frac{\partial^2 E}{\partial\theta^2}\frac{\partial^2 E}{\partial\phi^2}-\left[\frac{\partial^2 E}{\partial\theta\,\partial\phi}\right]^2\right] . \quad (5)$$

The second derivatives must be evaluated for equilibrium values of θ and ϕ. We thus obtain the following resonance expression:

$$(\omega/\gamma)^2=[H\cos(\phi_H-\phi)-4\pi M_{\rm eff}\sin^2\phi+(K_1/M)(2-\sin^2 2\phi)]\times[H\cos(\phi_H-\phi)+4\pi M_{\rm eff}\cos 2\phi+(2K_1/M)\cos 4\phi] . \quad (6)$$

The best fits between the experimental and calculated data were obtained using the parameters shown in Table I. Bulk values for g were used in the fitting ($g_{\rm Co}=2.18$; $g_{\rm Fe}=2.10$; and $g_{\rm Ni}=2.21$). For all the Co films, the in-plane angular dependence of the FMR field is relatively flat around the $\langle 110 \rangle$ easy axis but quite sharply peaked around the $\langle 100 \rangle$ hard axis. This angular dependence is more clearly shown in Fig. 7 for a 100-Å Co film. We see a similar, but less pronounced, effect in the Ni films. As described by Eqs. (2) and (3), this is due to the saturation magnetization not being collinear with the in-plane dc magnetic field.[28] Except for the Ni films with thicknesses <100 Å, all the samples had similar in-plane anisotro-

TABLE I. Summary of FMR (12 GHz) data on magnetic films grown on Cu(100)/Si(100).

Sample	$4\pi M_{\rm eff}$ (kG)	K_1/M (kG)	Linewidth ΔH[a] (G)	H_u[b] (kG)
500-Å Ni	1.5	−0.22	700	4.6
100-Å Ni	0.0	−0.30	1300	6.1
50-Å Ni[c]	−1.8	−0.50	1300	7.9
500-Å Co	17.6	−0.17	150	0.0
100-Å Co	14.3	−0.33	250	3.3
25-Å Co	14.4	−0.43	560	3.2
500-Å Fe	18.1	0.14	300	3.3
100-Å Fe	15.6	0.13	80	5.8
50-Å Fe	13.6	0.11	90	7.8
30-Å Fe	9.8	0.09	190	11.6

[a]Along the easy axis of magnetization.
[b]The perpendicular uniaxial field is defined as $H_u=4\pi M_s-4\pi M_{\rm eff}$. Bulk values of $4\pi M_s$ were used: 6.08 kG (Ni), 17.6 kG (Co), and 21.45 kG (Fe).
[c]From out-of-plane measurements.

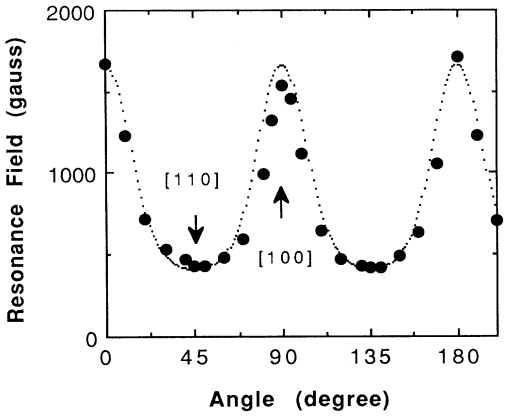

FIG. 7. The angular dependence of the in-plane FMR resonance field for a 100-Å Co film. The dotted curve was generated using the parameters given in Table I.

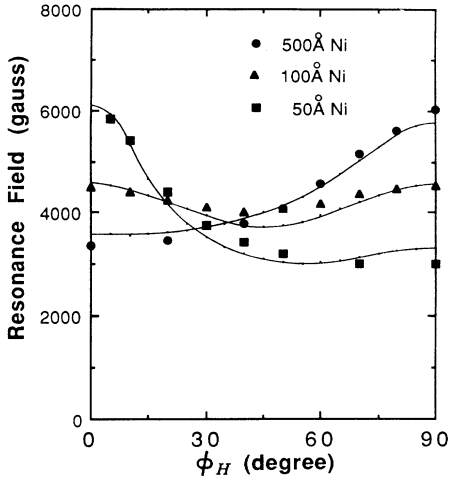

FIG. 8. The out-of-plane FMR measurements for Ni films (resonance field vs ϕ_H). The solid lines correspond to fitted data using the parameters in Table I.

pies to that of the 500-Å-thick films. For Fe films thicker than 30 Å, the FMR K_1 values represent a net anisotropy which is an average over the four possible orientations of the Fe(110) grains, leading to a fourfold in-plane anisotropy. In other words, these values are not intrinsic to Fe, but only to this particular arrangement of the Fe(110) grains.

A very weak and broad in-plane FMR signal was observed for the 50-Å Ni film. However, out-of-plane FMR measurements on the same film showed a very clear FMR absorption with the applied field normal to the plane of the film. This resonance moves to higher fields as the applied magnetic field is rotated away from the normal. Figure 8 is a plot of the resonance field versus ϕ_H for Ni films of thickness of 500, 100, and 50 Å. The solid lines are fits using Eqs. (4) and (6). The 50-Å Ni film has a negative value for $4\pi M_{\text{eff}}$, due to a strong uniaxial perpendicular anisotropy field which overcomes the demagnetizing field. For this film, the easy magnetic axis lies perpendicular to the plane of the film.

Assuming bulk values for $4\pi M_s$, Table I lists the perpendicular uniaxial fields (H_u) for all the samples. In general, H_u increases as the film thickness decreases. Plotting H_u vs 1/thickness, we observe straight-line graphs with nonzero intercepts for Ni and Fe films, but not for the Co samples. As was pointed out by Néel,[29] the symmetry breaking present at an interface can lead to a contribution to H_u which is inversely proportional to the thickness (the so-called magnetocrystalline surface anisotropy). However, surface roughness present in these films can also affect the values of H_u.[13,30] The roughness can give rise to an effective positive dipolar surface anisotropy, reducing the value of $4\pi M_{\text{eff}}$. At present, we do not have a quantitative estimation of the roughness of our films. X-ray reflectivity measurements could be used to obtain such information.

We also cannot rule out the contribution from a stress-induced magnetic anisotropy due to the epitaxial strains induced in the films by the substrate. All three systems studied, Ni(100)/Cu(100), Co(100)/Cu(100), and Fe(110)/Cu(100) are subjected to tensile strain between the magnetic metal and the Cu due to the smaller bulk lattice constants of the magnetic metals. This can lead to a stress-induced magnetic anisotropy due to inverse magnetostriction. However, as the thickness is increased, it is thought that the epitaxial strains are relieved by misfit dislocations. In the following, we will show that for the Ni samples, a stress-induced magnetic anisotropy may be the major contribution to the observed perpendicular anisotropy for a thickness of 50 Å.

X-ray analysis of Ni(100)/Cu(100) films grown under similar conditions has shown distorted Ni lattices, where Ni is under tensile stress in the plane parallel to the interface, and an associated perpendicular compressive stress.[24] An estimation of K_u can be made using the following expression:[31]

$$K_u = 3/2\lambda_{100}(C_{11}-C_{12})(\varepsilon_\perp-\varepsilon_\parallel)\ , \tag{7}$$

where $\varepsilon_\perp$ and $\varepsilon_\parallel$ are the perpendicular and parallel strains, respectively, λ_{100} is the magnetostriction constant along [100], and C_{11} and C_{12} are the cubic elastic stiffness constants. The above expression is derived for a $\langle 100 \rangle$ surface-oriented film by writing the magnetoelastic energy as a function of the elastic strains and the direction cosines of the magnetization, both of which are expressed relative to the cubic reference frame of the film. For Ni samples of thicknesses 500, 100, and 50 Å, grown under similar conditions, $\varepsilon_\perp$ and $\varepsilon_\parallel$ are given in Ref. 24. For the above samples $(\varepsilon_\perp-\varepsilon_\parallel)$ are -0.87%, -1.24%, and -2.43%, respectively. For Ni, using the following bulk values[31] $M_s=485$ emu/cm^3, $\lambda_{100}=-45.9\times10^{-6}$, $C_{11}=2.5\times10^{12}$ dyn/cm^2, and $C_{12}=1.6\times10^{12}$ dyn/cm^2, we calculate H_u to be 2.22, 3.17, and 6.21 kG for the 500, 100, and 50 Å samples, respectively. A comparison of the calculated and experimentally determined values of H_u (Table I) indicates that the major contribution to H_u in the 50-Å Ni film is due to inverse magnetostriction, whereas for the 100-Å and 500-Å Ni samples inverse magnetostriction can account for only about half of the

observed H_u. Surface roughness and the breaking of the symmetry at the interface may account partly for this discrepancy, although these effects become relatively smaller as the thickness increases. Further study of the microstructure of these Ni films will, perhaps, lead to a clearer understanding of the observed values of H_u.

In summary, we have used x-ray and RHEED measurements to confirm the epitaxial growth of Cu(100) on Si(100) with a 45° rotation. The growth of Cu is dominated by three-dimensional growth. Epitaxial growth of the magnetic metals was observed using RHEED, with Ni and Co growing with a fcc (100) structure, whereas Fe grows with a bcc(110) Pitsch orientation relationship. FMR confirms the various crystallographic analyses. We observed with FMR that the easy and hard in-plane magnetic axes of Ni and Co are along [110] and [100], respectively, whereas in Fe the easy and hard magnetic axes are parallel to Cu[100] and [110], respectively. The FMR data were analyzed by solving the energy-density expression under equilibrium and resonance conditions, obtaining values of the uniaxial perpendicular anisotropy field H_u. The observed H_u fields are explained as being partly due to both roughness-induced positive surface dipolar anisotropy and stress-induced magnetic anisotropy via inverse magnetostriction. However, the large perpendicular anisotropy observed for the 50 Å Ni film is accounted for as due mainly to the latter effect.

ACKNOWLEDGMENTS

This research was funded, in part, by National Science Foundation Grant No. DMR-9120274. The authors thank K. Fang and U. Rao for their contributions to the FMR measurements and B. Demczyk for the TEM measurements. One of the authors (R.N.) wishes to acknowledge helpful discussions with B. Heinrich on FMR and B. M. Clemens on strain-induced anisotropy.

[1]B. Heinrich, K. B. Urquhart, A. S. Arrott, J. F. Cochran, K. Myrtle, and S. T. Purcell, Phys. Rev. Lett. **59**, 1756 (1987).
[2]C. Chappert, K. LeDang, P. Beauvillain, H. Hurdequint, and D. Renard, Phys. Rev. B **34**, 3192 (1986).
[3]G. A. Prinz, G. T. Rado, and J. J. Krebs, J. Appl. Phys. **53**, 2087 (1982).
[4]J. J. Krebs, B. T. Jonker, and G. A. Prinz, J. Appl. Phys. **61**, 2596 (1987).
[5]S. A. Oliver, C. Vittoria, J. J. Krebs, B. T. Jonker, and G. A. Prinz, J. Appl. Phys. **65**, 2799 (1989).
[6]B. T. Jonker, J. J. Krebs, and G. A. Prinz, J. Appl. Phys. **64**, 5340 (1988).
[7]B. Heinrich, J. F. Cochran, A. S. Arrott, S. T. Purcell, K. B. Urquhart, J. R. Dutcher, and W. F. Egelhoff, Jr., Appl. Phys. A **49**, 473 (1989).
[8]A. Layadi, J. O. Artman, B. O. Hall, R. A. Hoffman, C. L. Jensen, D. J. Chakrabarti, and D. A. Saunders, J. Appl. Phys. **64**, 5760 (1988).
[9]Z. Zhang, P. E. Wigen, and S. S. P. Parkin, J. Appl. Phys. **69**, 5649 (1991).
[10]J. O. Artman, D. J. DeSmet, X. Shao, J. C. Cates, C. Alexander, Jr., M. R. Parker, E. T. Lacey, D. G. Lord, and P. J. Grundy, J. Appl. Phys. **70**, 6038 (1991).
[11]R. Krishnan, J. Magn. Magn. Mater. **50**, 189 (1985).
[12]J. P. Renard and P. Beauvillain, Phys. Scr. T **19**, 405 (1987).
[13]P. Bruno and J. P. Renard, Appl. Phys. A **49**, 499 (1989).
[14]G. S. Higashi, R. S. Becker, Y. J. Chabal, and A. J. Becker, Appl. Phys. Lett. **58**, 1656 (1991).
[15]Chin-An Chang, J. Appl. Phys. **67**, 566 (1990).
[16]Chin-An Chang, Phys. Rev. B **42**, 11 946 (1990).
[17]Chin-An Chang, Appl. Phys. Lett. **57**, 2239 (1990).
[18]R. Naik, C. Kota, and B. Demczyk (unpublished).
[19]J. Koike and M. Nastasi, in *Evolution of Thin Film and Surface Microstructure,* edited by C. V. Thompson, J. Y. Tsao, and D. J. Srolovitz, MRS Symposia Proceedings No. 202 (Materials Research Society, Pittsburgh, 1991), p. 13.
[20]M. Kato, S. Fukase, A. Sato, and T. Mori, Acta Metall. **34**, 1179 (1986).
[21]M. Kato, M. Wada, A. Sato, and T. Mori, Acta Metall. **37**, 749 (1989).
[22]U. Dahmen, Acta Metall. **30**, 63 (1982).
[23]C. Kota, R. Naik, and B. Demczyk (unpublished).
[24]Chin-An Chang, J. Appl. Phys. **68**, 4873 (1990).
[25]Chin-An Chang, Appl. Phys. Lett. **58**, 1745 (1991).
[26]J. O. Artman, Phys. Rev. **105**, 74 (1957).
[27]J. Smit and H. C. Beljers, Phylips Res. Rep. **10**, 1113 (1955).
[28]B. Heinrich, S. T. Purcell, J. R. Dutcher, K. B. Urquhart, J. F. Cochran, and A. S. Arrott, Phys. Rev. B **38**, 12 879 (1988).
[29]P. Bruno, J. Appl. Phys. **64**, 3153 (1988).
[30]L. Néel, J. Phys. Rad. **15**, 376 (1954).
[31]S. Chikazumi and S. H. Charap, *Physics of Magnetism* (Wiley, New York, 1964).

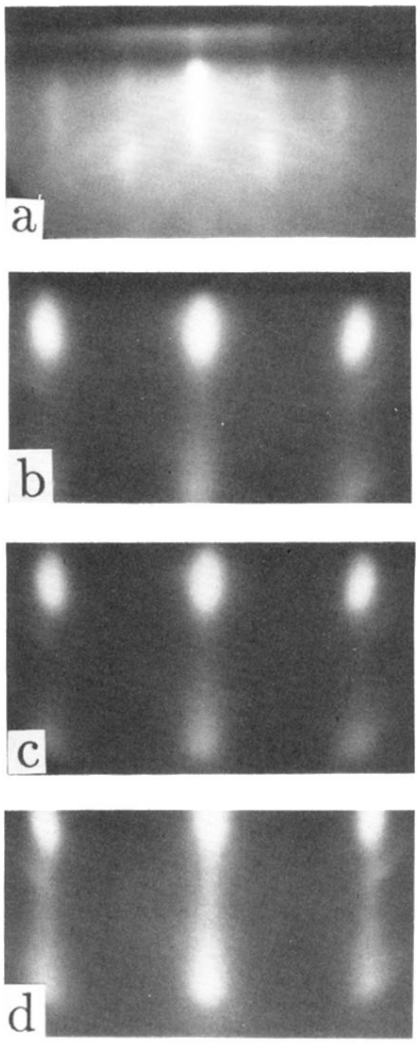

FIG. 1. RHEED patterns: (a) obtained from a clean Si(100) surface, (b) after a 500-Å Cu deposition, (c) after a 500-Å Co deposition on a 500-Å Cu seed layer, and (d) after a 500-Å Ni deposition on a 500-Å Cu seed layer. All patterns are taken along a Si⟨110⟩ azimuth with an electron beam of energy 15 keV.

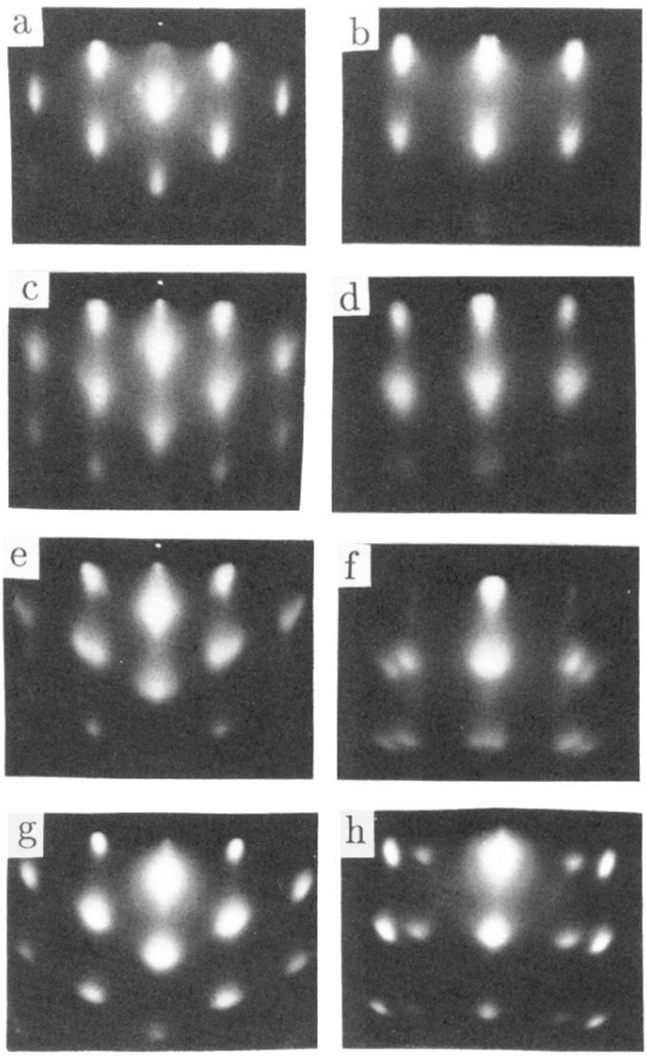

FIG. 3. RHEED data for an Fe deposition on Cu(100)/Si(100). (a) and (b) show patterns for a 1500-Å Cu(100) seed layer; (c) and (d) after a 10-Å Fe deposition; (e) and (f) after a 50-Å Fe deposition; (g) and (h) after a 500-Å Fe deposition. (a), (c), (e), and (g) are along a Si⟨100⟩ azimuth; (b), (d), (f), and (h) are along a Si⟨110⟩ azimuth.